ADVANCED OPTICAL MATERIALS

www.advopticalmat.de

Carbon-Bridged *p*-Phenylenevinylene Polymer for High-Performance Solution-Processed Distributed Feedback Lasers

Marta Morales-Vidal, José A. Quintana, José M. Villalvilla, Pedro G. Boj, Hiroki Nishioka, Hayato Tsuji, Eiichi Nakamura,* Guy L. Whitworth, Graham A. Turnbull, Ifor D. W. Samuel, and María A. Díaz-García**

Thin-film organic lasers are attractive light sources for a variety of applications. Recently, it is reported that carbon-bridged oligo(*p*-phenylenevinylene)s (COPV*n* with repeating unit *n* = 1–6) function as unique laser dyes which combine high fluorescence efficiency, wavelength tunability, and both thermal and photostability, making them ideal for use in organic semiconductor lasers. However, in order to obtain such excellent properties, COPV*n* require blending in a matrix, such as a thermoplastic polymer, thus leading to miscibility issues, limited absorption, and charge transporting properties. Here, high-performance lasers with a novel active polymer poly-COPV1, based on the basic unit of COPV1 and prepared as a high-quality neat film, are reported which overcome the trade-off between the device performance and durability. The prepared lasers show thresholds 30 times lower and operational lifetimes 300 times longer than devices based on COPV1 dispersed in polystyrene. The low threshold operation allows the poly-COPV1 lasers to be pumped by a nitride diode laser.

1. Introduction

Distributed feedback (DFB) lasers with both the active material and the resonator made of solution-processable materials have recently attracted great attention for their potential as inexpensive and high-throughput lasers.[1,2] Their interest lies in the prospect to obtain low-cost, mechanically flexible, wavelength tunable, compact lasers with easy integration to other devices. Great progress has been made in improving both the active laser material and the DFB resonator, including aspects such as efficiency, stability, easy processing, and integrability.[1,2] There have also been advances on the application of these devices to different areas, including optical communications,[3] spectroscopy,[4] and sensing.[5–7]

The choice of active organic material is crucial to obtaining high laser performance. It should simultaneously achieve various characteristics such as high-quality films with strong photoabsorption (and hence high gain), high photoluminescence quantum yield (PLQY), low waveguide loss, and high photostability. In previous work, it was demonstrated that carbon-bridged oligo(*p*-phenylenevinylene) dyes (COPV*n*, with *n* = 1–6), dispersed in polystyrene (PS), are among the best dyes to be used for DFB lasers emitting at wavelengths that cover a wide range of the visible spectrum (380–600 nm).[8–10] Films doped with COPV*n*, with between 3 and 6 repeat units (*n*), emitting within the 515–585 nm spectral range, exhibited very low amplified spontaneous emission (ASE) and DFB pump intensity thresholds (down to 0.7 kW cm^{-2}) and very long operational lifetimes (up to 10^6 pump pulses (pp)).

A drawback of COPV*n* compounds is that in order to obtain good quality films with high performance they require blending with another material (i.e., a thermoplastic polymer such as PS), thus leading to limited absorption and charge-transporting

Dr. M. Morales-Vidal,[+] Dr. J. M. Villalvilla, Prof. M. A. Díaz-García
Dpto. Física Aplicada
Instituto Universitario de Materiales de Alicante (IUMA)
and Unidad Asociada UA-CSIC
Universidad de Alicante
Alicante 03080, Spain
E-mail: maria.diaz@ua.es

The ORCID identification number(s) for the author(s) of this article can be found under https://doi.org/10.1002/adom.201800069.

[+]Present address: Grupo de Investigación en Aplicaciones del Láser y Fotónica, Dpto. Física Aplicada, University of Salamanca, Salamanca E-37008, Spain

[++]Present address: Department of Chemistry, Faculty of Science, Kanagawa University, 2946 Tsuchiya, Hiratsuka 259-1293, Japan

DOI: 10.1002/adom.201800069

Dr. J. A. Quintana, Dr. P. G. Boj
Dpto. Óptica
IUMA and Unidad Asociada UA-CSIC
Universidad de Alicante
Alicante 03080, Spain

H. Nishioka, Prof. H. Tsuji,[++] Prof. E. Nakamura
Department of Chemistry
School of Science
The University of Tokyo
Hongo, Bunkyo-ku, Tokyo 113-0033, Japan
E-mail: tsujiha@kanagawa-u.ac.jp; nakamura@chem.s-u-tokyo.ac.jp

Dr. G. L. Whitworth, Prof. G. A. Turnbull, Prof. I. D. W. Samuel
Organic Semiconductor Centre
SUPA
School of Physics and Astronomy
University of St Andrews
St Andrews KY16 9SS, UK

properties (important for the future prospect of an electrically pumped laser) and potential miscibility issues.

Here, we report a COPV-based polymer (i.e., poly-COPV1, see chemical structure in **Scheme 1**) which shows an excellent laser performance when prepared as a uniform neat film. To develop a suitable COPV-polymer, one needs to consider both the structural rigidity of the chromophore and the solubility of the polymer. The latter requires some flexibility of the chain. For this reason, and also to benefit from its easier synthesis, we selected COPV1 for polymerization, from the previously reported COPV*n* compounds.

Now, while the longer chain oligomers achieved excellent laser performance, COPV1 showed weaker ASE performance, with a rather high threshold of 90 kW cm^{-2} and a lifetime of only 1.8×10^2 pp. The instability problems were attributed to the reactive terminal sites of the photoexcited states.[11] In this work, our hypothesis is that through polymerization, the terminal sites of COPV1 would be protected (in a similar way to the longer COPV homologues which have a smaller distribution of terminal sites and thus higher photostability) so its photostability would improve. Moreover, the resulting polymer is expected to benefit from the improvement of the tradeoff between absorbance and PLQY of the active layer upon increasing concentration, first because the long alkyl chains would keep the active units separated from each other to prevent intermolecular PL quenching; second, because the rigidity and well-defined structure of the COPV unit would prevent the existence of nonradiative decay by intrachain energy transfer, unlike traditional phenylenevinylenes which may be randomly segmented.

For efficient and high-performance DFB lasers, we have also examined the selection of an efficient DFB architecture. Typical state-of-the-art organic DFB lasers have shown pump thresholds of <1 kW cm^{-2}, traditionally with the gratings engraved into conventional inorganic substrates (e.g., SiO_2), onto which the active film is deposited.[1,2] Efforts aiming at reducing device costs and improving mechanical flexibility have focused on architectures with gratings imprinted directly on the active film (e.g., thermal or solvent imprinting),[12–15] or devices wherein both the active material and the resonator can be processed from solution (such as UV-nanoimprint lithography (UV-NIL)).[9,16–20] Recently, an important landmark was the demonstration of lasers with high efficiency, low threshold, long operational lifetime, and broad wavelength tunability in a single device, thanks to the combination of highly efficient and photostable dyes and a not very common DFB resonator configuration.[9] This consisted on a resist layer with the grating engraved by holographic lithography (HL) and deposited on top of an active film of uniform thickness. Another remarkable milestone in resonator design was the fabrication of DFB lasers using substructured gratings, achieving much lower thresholds (i.e., <0.1 kW cm^{-2}).[21] The key advantage of substructured gratings, which consist of gratings with an additional ridge in the unit cell, is that they allow separate optimization of feedback along the waveguide and output coupling in a direction perpendicular to the film plane, thus lowering the lasing threshold.

In this paper, we report organic thin-film lasers using a novel COPV-based polymer, poly-COPV1, prepared as a neat film without any matrix. The performance of the devices is much better than that of lasers based on monomeric COPV1 dispersed in thermoplastic polymers. The ASE threshold is 30 times lower and the ASE lifetime 300 times longer than for the monomer COPV1, reaching values similar to those obtained with COPV3. Efficient and high-performance DFB lasers, with both active material and resonator made of polymeric material, have been prepared by following recently reported successful strategies, such as the use of a top-layer polymeric resonator architecture or the employment of a substructured grating.

2. Results

2.1. Synthesis of Poly-COPV1

The synthesis of poly-COPV1 is shown in Scheme 1. COPV1-Br_2 was synthesized by a procedure previously reported,[22] and was subjected to borylation to obtain COPV1-$(Bpin)_2$. The Suzuki–Miyaura coupling polymerization of COPV1-Br_2 and COPV1-$(Bpin)_2$ proceeded smoothly to give poly-COPV1 in 80%

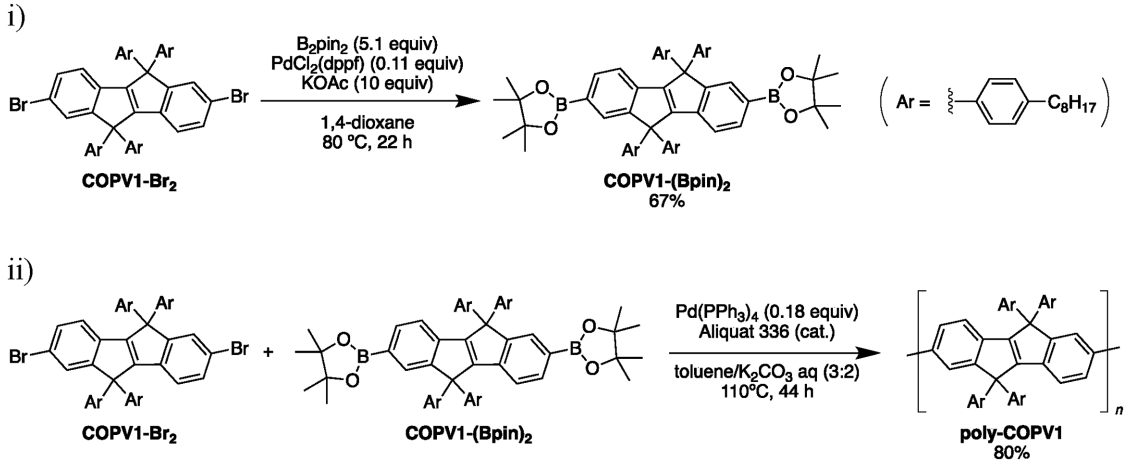

Scheme 1. Synthetic procedures to prepare COPV1-$(Bpin)_2$ (i) and poly-COPV1 (ii).

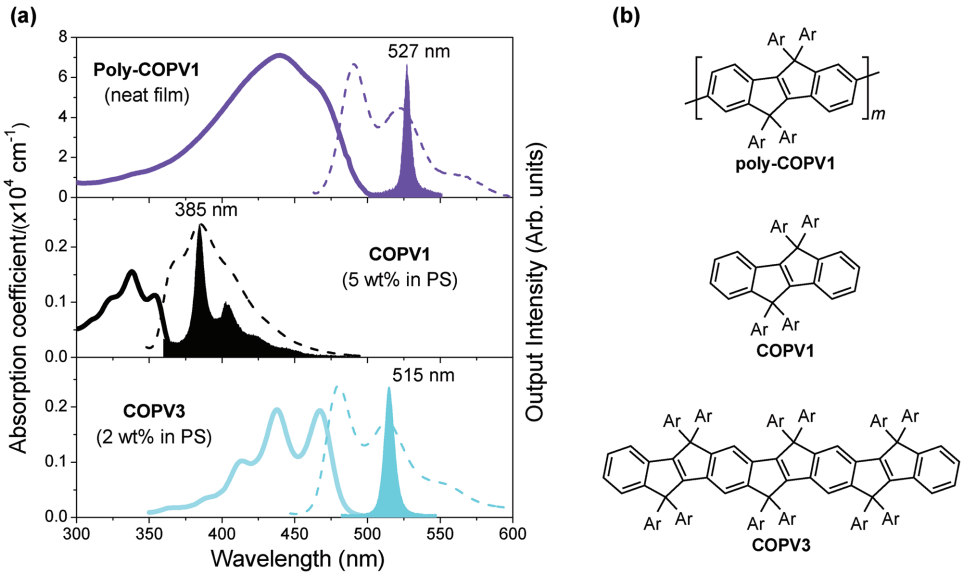

Figure 1. Optical properties of a poly-COPV1 neat film, compared to polystyrene films doped with either 5 wt% of COPV1 or 2 wt% of COPV3. a) Absorption coefficient, α (solid line, left axis), photoluminescence intensity (dashed line, right axis), and amplified spontaneous emission, ASE, intensity (filled area, right axis), versus wavelength, λ. b) Chemical structures of poly-COPV1, COPV1, and COPV3, from top to bottom.

yield. Poly-COPV1 was readily soluble in common organic solvents, such as toluene, tetrahydrofuran (THF), and chloroform.

2.2. Poly-COPV1 Neat Films: Absorbance, PL, and ASE Properties

Taking advantage of the good solubility of poly-COPV1, neat films with high optical quality were prepared by spin-coating from a toluene solution. The optical properties of the films are shown in **Figure 1**, with key parameters relevant to laser operation listed in **Table 1**. The polymer has a peak absorption at 440 nm with a shoulder around 470 nm. The absorption coefficient at the pumping wavelength ($\alpha[\lambda_{pump}]$) of a poly-COPV1 thin film was 6.67×10^4 cm^{-1}, which is 40 times larger than those of previously reported for COPV-dispersed PS films. Poly-COPV1 showed efficient PL with spectral peaks at 490 and 525 nm, and a high PLQY of 68%, even in a neat film. Both the high absorbance and high PLQY offer a significant improvement on the monomeric COPVs dispersed in PS in previous work.[8]

It should be noted about the significant red-shift of the absorption and PL spectra of the poly-COPV1 film with respect to those of COPV1 dispersed in PS. This shift is due to the electronic interaction between the COPV1 units in the polymer chain (dihedral angle between the monomers: ≈37°, according to calculations). The existence in the poly-COPV1 film of

Table 1. Optical and ASE properties of films without gratings (data for COPV1 and COPV3 extracted from ref. [8]).

	Poly-COPV1 neat film	COPV1, 5 wt% in PS	COPV3, 2 wt% in PS
Substrate	Glass BK7 (s1); Fused silica (s2)	Fused silica	Fused silica
$n^{a)}$ (at λ_{ASE})	1.68	1.64	1.60
$h^{b)}$ [nm]	250 (s1); 600 (s2)	720	650
$\lambda_{ABS\_max}{}^{c)}$ [nm]	440	323, 338, 352	413, 437, 467
PLQY$^{d)}$ [%]	68	100	100
$\lambda_{pump}{}^{e)}$ [nm]	450 (s1); 436 (s2)	355	436
α (at λ_{pump})$^{f)}$ [cm^{-1}]	6.67×10^4	1.88×10^3	1.91×10^3
$\lambda_{ASE}{}^{g)}$ [nm]	527.3 (s1); 528.6 (s2)	385.2	514.8
$I_{th\text{-}ASE}{}^{h)}$ [kW cm^{-2}]	3.0 (s1); 4.0 (s2)	90	4.0
$\tau_{1/2}{}^{ASE}$ [pump pulses]/$I_{pump}{}^{i)}$ [kW cm^{-2}]	7.7×10^4/9.8 (s1); 6.0×10^4/18 (s2)	1.8×10^2/198	8.4×10^4/8 7.8×10^3/1800
$FWHM_{ASE}{}^{j)}$ [nm]	5	6	8

[a)]Refractive index (error ≈ 1%); [b)]Film thickness (error ≈2%); [c)]Peak absorption wavelengths; [d)]PLQY: Photoluminescence quantum yield (error ≈10%); [e)]Pump wavelength; [f)]Absorption coefficient at λ_{pump}; [g)]ASE wavelength (error is ±0.5 nm); [h)]ASE threshold (error ≈ 10%, estimated statistically as the standard deviation from measurements on several nominally identical samples); [i)]ASE photostability half-life under indicated I_{pump} at 10 Hz pump (error ≈ 10%, estimated same as above); [j)]ASE linewidth, defined as the full width at half of the maximum (error is ±1 nm).

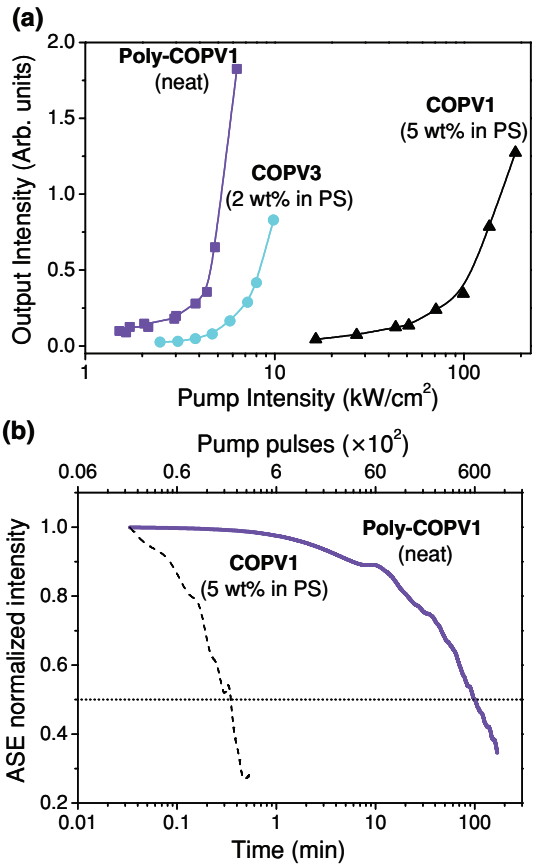

Figure 2. Amplified spontaneous emission (ASE) performance of a poly-COPV1 neat film and comparison to a COPV1-doped (at 5 wt%) polystyrene film. a) Output intensity versus pump intensity, for ASE threshold determination. b) ASE intensity versus time, for ASE photostability half-life determination. The pump intensity is six and two times above threshold for poly-COPV1 and COPV1, respectively.

self-absorption ("inner filter effect") does not seem to be significant according to the small difference between the spectra of poly-COPV1 as a neat film and as a highly diluted liquid solution (see Figure S1, Supporting Information). As a consequence, the PLQY of the neat film remains as high as that of the dilute solution (68 and 79%, for film and solution, respectively). The refractive index (n_f) and the extinction coefficient (k) as a function of wavelength for the poly-COPV1 film were determined by ellipsometry (see Figure S2, Supporting Information). The specific n_f value at the wavelength at which ASE emission appears (λ_{ASE}) is included in Table 1.

Under optical excitation at λ_{pump} = 450 nm, the poly-COPV1 shows ASE at λ_{ASE} = 527 nm (see Figure 1), which corresponds to the wavelength of the first vibronic PL peak, as generally occurs for very planar compounds with high PLQY and small Stokes shifts. Its ASE threshold ($I_{th\text{-}ASE}$) is very low (3 kW cm^{-2}, see **Figure 2**a and Table 1), being this value 30-fold lower than that obtained with a COPV1-doped PS film, and similar to that obtained with a COPV3-doped PS film.[8] Note that some of the measurements performed on the poly-COPV1 film (i.e., those of sample labeled as S2 in Table 1) were performed under the same experimental conditions used to characterize COPV3 (excitation at λ_{pump} = 436 nm), to enable proper comparison of both materials.

The most remarkable property of poly-COPV1 is its substantially increased photostability compared with that of the monomer. The ASE half-life, $\tau_{1/2\text{-}ASE}$, was measured under excitation at a pump intensity (I_{pump}) of 20 kW cm^{-2} (i.e., six times above threshold) under ambient conditions directly on the film (i.e., nonencapsulated or protected). From plots of the ASE intensity versus time (see Figure 2b) we find $\tau_{1/2\text{-}ASE} = 6 \times 10^4$ pp. This value is more than 300 times larger than that obtained from a 5 wt% COPV1-doped PS film under an excitation of two times threshold (I_{pump} = 180 kW cm^{-2}) (see Figure 2b).[8] Importantly, the photostability of poly-COPV1, which is prepared as a neat film, is outstanding, not just in comparison to the monomer COPV1, but also in comparison to other COPVs. For example, COPV3 dispersed at 2 wt% in PS showed a $\tau_{1/2\text{-}ASE}$ value of 8.4×10^4 pp, similar to that obtained with the poly-COPV1 film, but with softer pumping conditions (I_{pump} = 8 kW cm^{-2}, two times above threshold) and with a very low doping level. Note that the longest ASE lifetime reported for COPVs was for COPV6 ($\tau_{1/2\text{-}ASE} = 1 \times 10^6$ pp), when the dye doping concentration was 2 wt%, however the stability decreased considerably for higher concentrations ($\tau_{1/2\text{-}ASE} = 3 \times 10^4$ pp for 20 wt%).[8]

The high photostability shown by the poly-COPV1 neat film indicates that our polymerization strategy has been successful in protecting the COPV1 terminal sites from chemical reactions. From the viewpoint of steric effect, the central moiety of the COPV1 molecule is sterically protected by the aromatic substituents with long alkyl chains (Ar) on the bridging carbon atoms, whereas the terminal benzene rings are not. From the viewpoint of molecular orbitals (see Figure S3, Supporting Information), both HOMO (π) and LUMO (π^*) are delocalized over the whole molecule, and its photoexcited $\pi\pi^*$ state has a greater contribution of quinoidal resonance structure than the ground state, resulting in unprotected dangling bonds at their terminal sites that are liable to react with other species (e.g., molecular oxygen or neighboring COPV molecules). Like longer COPV homologues that have smaller distribution on the terminal sites and thus higher photostability, polymeric COPV1 excludes this terminal effect to give much higher photostability, in accordance with the initial hypothesis.

Net gain coefficients (g) of 60 and 33 cm^{-1}, at I_{pump} of 34.8 and 18.2 kW cm^{-2}, respectively, were determined for the poly-COPV1 film by means of a variable stripe length study (see Figure S4, Supporting Information).[23] These g values are superior to those reported for a 8 wt% COPV6-doped PS film (60 and 6.3 cm^{-1}, at I_{pump} of 43.3 and 11.5 kW cm^{-2}, respectively,[8] and only about twice lower than state-of-the-art organic semiconductors.[24,25]

3. DFB Lasers Based on Poly-COPV1 Films

DFB lasers based on poly-COPV1 neat active films and different types of device architectures were subsequently fabricated. All the resonators consisted of 1D relief gratings (with single period or substructured) imprinted in a polymeric layer.

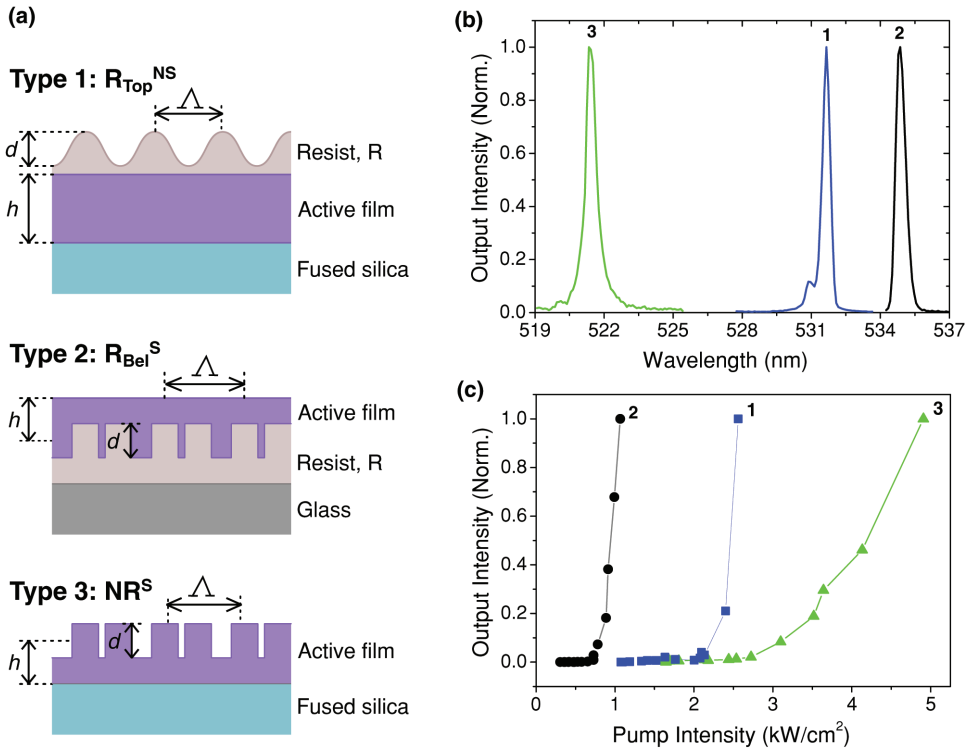

Figure 3. DFB lasers based on poly-COPV1. a) Schemes of DFB laser types fabricated (from top to bottom): **Type 1**: $\mathbf{R_{Top}}^{\mathbf{NS}}$, top-layer resist resonator with single period (not substructured); **Type 2**: $\mathbf{R_{Bel}}^{\mathbf{S}}$, substructured grating imprinted in resist layer located below the active film; **Type 3**: $\mathbf{NR}^{\mathbf{S}}$, substructured grating imprinted over active film; no resist is used. b) Spectra for selected lasers of the various types: $\mathbf{R_{Top}}^{\mathbf{NS}}$ (**1**), $\mathbf{R_{Bel}}^{\mathbf{S}}$ (**2**), and $\mathbf{NR}^{\mathbf{S}}$ (**3**); their geometrical parameters are listed in Table 2. c) Output intensity versus pump intensity curves for threshold determination, for the devices shown in (b). Symbols are data points and solid lines are guides to the eye.

Three types of architecture were studied: with a resist resonator located either below or on top of the active film, which we denote as R_{Bel} and R_{Top} architectures, respectively; and a device with no resist layer (denoted as NR) and with the grating (substructured) imprinted directly on the active film. According to this, the prepared lasers are classified into three categories (see **Figure 3**a):

Type 1: $\mathbf{R_{Top}}^{\mathbf{NS}}$ (not substructured top-layer resist resonator). Laser with a single period (i.e., not substructured) DFB grating engraved by HL on a photoresist (dichromated gelatine, DCG) layer deposited on top of the active film.

Type 2: $\mathbf{R_{Bel}}^{\mathbf{S}}$ (substructured resist resonator below the active film). Laser with a substructured grating, fabricated via UV-NIL on a mr-XNIL26 UV-NIL resist layer located below the active film.

Type 3: $\mathbf{NR}^{\mathbf{S}}$ (substructured resonator on active film, no resist). Laser with no resist and a substructured grating directly imprinted in the active film surface by means of solvent immersion imprint lithography (SIIL).

Figure 3b shows spectra from a selection of lasers (one for each resonator type) whose emissions appear at wavelengths in the spectral range between 521 and 535 nm. Single mode emission was obtained in all cases, with linewidths of around 0.5 nm or below. The geometrical parameters of these DFB lasers are listed in **Table 2**, along with their lasing characteristics.

In order to compare the laser threshold performance to that of previously reported devices based on molecular COPV compounds (all with single period gratings), we first focus on device $\mathbf{R_{Top}}^{\mathbf{NS}}$ (**1**). Its emission (λ_{DFB} = 531.9 nm) is close to λ_{ASE}, with a laser threshold of 1.9 kW cm^{-2}. This value is significantly lower than that of previously reported devices based on COPV1 dispersed in PS with gratings engraved on inorganic substrates.[8] Importantly, the threshold obtained for device $\mathbf{R_{Top}}^{\mathbf{NS}}$ (**1**) is around the same than that obtained with the best lasers with a top-layer resonator architecture based on COPV3, emitting in similar spectral region.[9]

The benefit of using substructured gratings for poly-COPV1 lasers is illustrated by the results obtained with device $\mathbf{R_{Bel}}^{\mathbf{S}}$ (**2**), which showed the lowest threshold (0.7 kW cm^{-2}; see Figure 3c and Table 2). This device, which was optically pumped by a nitride diode laser, emitted at 534.9 nm, relatively close to the wavelength at which the gain is maximum (λ_{ASE} = 527 nm). We prepared other $\mathbf{R_{Bel}}^{\mathbf{S}}$ **type** lasers (see Table S5, Supporting Information) emitting at wavelengths further away (by around 15 nm) from λ_{ASE}, but they still show low thresholds (between 1 and 2 kW cm^{-2}).

Finally, device $\mathbf{NR}^{\mathbf{S}}$ (**3**), with the grating directly imprinted on the active film and no resist layer, was observed to emit at λ_{DFB} = 521.3 nm, ≈6 nm shorter in wavelength than λ_{ASE}. The threshold of this laser (2.8 kW cm^{-2}) was slightly higher than those of the other devices. Nevertheless, it can be considered low, taking into account that losses due to self-absorption are

Table 2. Geometrical and performance parameters of selected poly-COPV1 DFB lasers.

Device type[a]	Substrate	Resonator material	Device label[b]	h[c] [nm]	Λ[d] [nm]	w[e] [nm]	x[f] [nm]	λ_{pump}[g] [nm]	λ_{DFB}[h] [nm]	$I_{th\text{-}DFB}$[i] [kW cm^{-2}]	FWHM[j] [nm]
$\mathbf{R_{Top}^{NS}}$	Fused silica	DCG[k]	**1**	405	331			450	531.9	1.9	<0.5
$\mathbf{R_{Bel}^{S}}$	Glass	mr-XNIL26 UV-NIL[l]	**2**	≈140	350	95	75	445	534.9	0.7	<0.5
$\mathbf{NR^{S}}$	Fused silica	Active film	**3**	100	350	95	75	450	521.3	2.8	<0.5

[a]Device types as defined in Figure 3a: **Type 1: $\mathbf{R_{Top}^{NS}}$** (top-layer resist resonator with single period (not substructured). **Type 2: $\mathbf{R_{Bel}^{S}}$** (substructured grating imprinted on resist layer located below the active film). **Type 3: $\mathbf{NR^{S}}$** (substructured grating imprinted over active film; no resist is used); [b]Number on the label refers to the device Type; [c]Film thickness (error is ±5 nm); [d]Grating period; [e]Width of the two ridges within the unit cell of a substructured grating; [f]Separation between the two ridges within the unit cell of a substructured grating; [g]Pump wavelength; [h]DFB wavelength (error is ±0.2 nm); [i]DFB threshold (error ≈ 10%, estimated statistically as the standard deviation from measurements on several nominally identical samples); [j]DFB linewidth, defined as the full width at half of the maximum (error is ±0.5 nm); [k]Dichromated gelatine photoresist; [l]Resist for nanoimprint lithography.

higher in the blue side of λ_{ASE}, thus DFB lasers emitting in those regions have generally higher thresholds.

With regards to the operational lifetime of the lasers, in accordance with the ASE photostability results described in the previous section, very long DFB half-life values were obtained, that is, $\tau_{1/2\text{-}DFB} \approx 1 \times 10^6$ pp for device $\mathbf{R_{Bel}^{S}}$ **(2)** under an excitation density of two times threshold, and slightly larger for the other devices.

4. Conclusions

We have reported the synthesis of a COPV-based polymer, poly-COPV1, and demonstrated its great potential as the active material for thin film organic lasers. The material can be prepared as a high-quality neat waveguide film with a relatively high refractive index (n = 1.68, at λ = 527 nm) without any host matrix. This has the advantages of higher pump absorption and simpler processing compared to previously described oligomeric COPV derivatives, which require mixing with another material such as a thermoplastic polymer to obtain a good quality film with good laser performance. The fact that the shortest COPV unit (COPV1), among the ones reported to date (COPVn with n = 1–6), has been used for polymerization, is a remarkable aspect because its synthesis is much simpler. The ASE properties of the poly-COPV1 film have been investigated and compared to those of COPV1 dispersed in polystyrene. Results have shown a much better performance for the poly-COPV1: an ASE threshold 30 times lower and an ASE lifetime 300 times longer. The significant enhanced photostability of poly-COPV1 with respect to COPV1 is a consequence of the polymerization strategy used, which has resulted in a decreased number of reactive sites. DFB lasers, with both active material and resonator made of the polymeric material were made with either a top-layer polymeric resonator architecture, or with a substructured grating imprinted on a resist layer located below the active film or directly on the active film. Thresholds as low as 0.7 kW cm^{-2}, under pumping with an inexpensive GaN laser diode, and operational lifetimes of 1×10^6 pump pulses were obtained for a device with a substructured grating imprinted in a resist layer, with a poly-COPV1 film deposited on top. Lasers with a top-layer resonator architecture also demonstrated low thresholds around 2 kW cm^{-2} with single period gratings. Overall, this study demonstrates the great potential of COPV-based polymers for laser applications. Further work will focus on device architectures combining both strategies, that is, substructured gratings with top-layer resonator architecture to obtain even lower thresholds, improved efficiencies, and the possibility to fabricate wavelength tunable devices within a single chip.[9] From the materials point of view, further work will focus on the development of other polymers, based on other COPV compounds, for example, to expand the emission of the devices to wavelength ranges further away to those accessible for poly-COPV1.

5. Experimental Section

Synthesis: COPV1-(Bpin)$_2$: A mixture of COPV1-Br$_2$ (887 mg, 0.80 mmol), bis(pinacolato)diboron (1.03 g, 4.1 mmol), dichloro[1,1′-bis(diphenylphosphino)ferrocene]palladium(II) dichloromethane adduct (72.3 mg, 0.089 mmol), and potassium acetate (813 mg, 8.3 mmol) in 1,4-dioxane (16 mL) were stirred at 80 °C for 22 h. Water was added to the mixture, which was then extracted with dichloromethane. The organic layer was dried with $MgSO_4$ and concentrated in vacuo. Silica gel column chromatography (eluent: hexane/dichloromethane = 9/1, 4/1 then 2/1) and the reprecipitation from dichloromethane and methanol afforded the title compound as a white solid (650 mg, 67%). ^{1}H NMR (500 MHz, $CDCl_3$): δ 0.87 (t, J = 7.2 Hz, 12H), 1.26–1.29 (m, 64H), 1.53–1.58 (m, 8H), 2.52 (t, J = 7.7 Hz, 8H), 7.01 (d, J = 8.0 Hz, 8H), 7.14 (d, J = 7.4 Hz, 2H), 7.20 (d, J = 8.6 Hz, 8H), 7.60 (d, J = 7.4 Hz, 2H), 7.83 (s, 2H); ^{13}C NMR (125 MHz, $CDCl_3$): δ 14.12, 22.66, 24.78, 29.26, 29.48, 29.52, 31.35, 31.90, 35.56, 62.40, 83.52, 120.50, 128.20, 128.43, 130.56, 133.94, 139.55, 141.31, 141.50, 156.90, 157.23. m.p. 203–206 °C. HRMS (APCI+) m/z Calcd $C_{84}H_{114}B_2O_4^+$ ([M$^+$]): 1206.8970; Found: 1206.8872.

Poly-COPV1: A mixture of COPV1-Br$_2$ (133 mg, 0.12 mmol), COPV1-(Bpin)$_2$ (144 mg, 0.12 mmol), tetrakis(triphenylphosphine)-palladium(0) (26.0 mg, 0.022 mmol), and Aliquat 336 (5 drops) in toluene (6.0 mL) and 2 M K_2CO_3 aqueous solution (4.0 mL) was stirred at 110 °C for 44 h. Bromobenzene (0.05 mL) was then added to reaction mixture and stirred at 110 °C for 8 h. 4,4,5,5-Tetramethyl-2-phenyl-1,3,2-dioxaborolane (0.05 mL) was added to reaction mixture and stirred at 110 °C for another 10 h. The reaction mixture was diluted with dichloromethane, and passed through a silica gel short column. The solvent was removed in vacuo. The crude mixture was purified by gel permeation chromatography (GPC; eluent: chloroform) to remove smaller molecules. Reprecipitation from dichloromethane and methanol, and washing the obtained solid with acetone gave the title compound as a yellow solid (184 mg, 80% based on COPV1 monomer). HPLC (GPC): M_n = 5792, M_w = 8098, PDI = 1.40.

Thin Film Preparation and Thickness Characterization: Neat films of poly-COPV1 (refractive index n = 1.68, at λ = 527 nm) were prepared by spin-coating over appropriate substrates using toluene as a solvent.

Particularly, 250 nm thick films (s1) were deposited on glass BK7 substrates with dimensions (2.5 × 2.5) cm^2, while 600 nm thick films (s2) were deposited on (2.5 × 2.5) cm^2 fused silica to measure absorbance, PL, PLQY, ASE, and gain. Film thickness was determined by a Veeco Dektak 150 profilometer on the center of the samples (measurements on other parts of the sample were carried out to account for the error, see Table 1).

DFB Fabrication: **Type 1: R_{Top}^{NS}** lasers were fabricated by recording a second-order relief grating in a DCG layer deposited on the top of the active film following the procedure described in ref. [9]. First, a poly-COPV1 thin film was coated onto a fused silica substrate from a toluene solution followed by deposition of a DCG photoresist layer. The active film surface was treated in an oxygen plasma for a few seconds to improve photoresist adherence. The thickness after the treatment was h = 405 nm. Then, a 1D grating with a period Λ = 331 nm was recorded in the DCG layer by HL, desensitized in a cool water bath and dry developed in an oxygen stream-plasma for selective etching.

A UV-nanoimprint lithography process was used, as described in detail elsewhere,[26] to fabricate the substructured DFB resonators of the **Type 2: R_{Bel}^{S}** devices prepared. In this case, the grating was imprinted in a 300 nm thick layer of the low refractive index (n = 1.37) mr-XNIL26 UV-NIL resist previously deposited (by spin coating) onto glass substrates. Then, poly-COPV1 films were subsequently spin-coated onto the UV-NIL gratings and then encapsulated with a layer of the fluorinated polymer CYTOP (n = 1.34). The grating structure consists of two ridges of width w, displaced by a distance x, within each second order unit cell, and with a periodicity Λ = 350 nm. For device R_{Bel}^{S} (**2**), w = 95 nm and x = 75 nm. The other R_{Bel}^{S} type devices were prepared using different stamps (see Figure S4, Supporting Information) as to obtain gratings with different w and x values (see Table S1, Supporting Information). These parameters determine the relative amount of first-order and second-order character of the grating.

The SIIL technique was used to fabricate **Type 3: NR^{s}** devices. A substructured grating was directly imprinted on the active film, as described by Vasdekis et al.,[27,28] using acetone as the imprinting solvent. The same perfluoropolyether stamp used to prepare device R_{Bel}^{S} (**2**) was employed in this case.

Optical Characterization: Absorption measurements were carried out in a Varian Cary 300 Bio UV–vis spectrophotometer. PL and PLQY measurements were performed with a Hamamatsu integrating sphere. The excitation source for most of the ASE and DFB experiments was an optical parametric oscillator (OPO) (pumped with a pulsed Nd:YAG laser) operating at the 450 nm wavelength (4 ns pulse width; 20 Hz repetition rate). Some ASE measurements (sample S2) were performed at the 436 nm wavelength provided by a Raman cell pumped with the 532 nm line of a Nd:YAG laser (10 nm pulse width, 10 Hz repetition rate). Device R_{Bel}^{S} (**2**), showing the lowest threshold, was pumped with a 445 nm diode laser (20 ns, 20 Hz). The diode laser setup was an assembled in-house consisting of a laser head from Roither LaserTechnick (LD-445-1000MG) which was attached to a PicoLAS driver board (LDP-V 50-100).

ASE characterization was performed by focusing the pump beam to a stripe (dimensions of 2.9 mm × 0.3 mm or 3.5 mm × 0.5 mm, for excitation at 450 or 436 nm, respectively) using a cylindrical lens onto the surface of an unpatterned (with no DFB grating) active film. Light emission was collected from the edge of the film at a high pump power density, using an Andor fiber coupled grating spectrograph. The energy of the pump pulses was controlled by using a polarizing filters system. The ASE photostability was studied by recording the ASE intensity as a function of time and quantified by means of the half-life parameter.

For the DFB laser measurements performed under excitation with the OPO, the pump beam was focused to an ellipse with a minor and major axis of 1.0 and 1.2 mm, respectively (measured with a Coherent Inc. Beam Profiler at the position of the polymer films). For the experiments using the laser diode as excitation source, the pump beam was shaped to a stripe of dimensions 2 mm × 0.6 mm. In all cases, the emitted laser light was collected in a direction perpendicular to the film surface using the spectrograph.

Supporting Information

Supporting Information is available from the Wiley Online Library or from the author.

Acknowledgements

The authors are grateful to Dr. Tom Wood for performing the spectroscopic ellipsometry measurements. The Spanish team acknowledges support from the Spanish Government (MINECO) and the European Community (FEDER) through Grant Nos. MAT2011-28167-C02-01 and MAT2015-66586-R. M.M-V. was partly supported by a MINECO FPI Fellowship (No. BES-2009-020747) and by a Junta de Castilla y León (JCYL) Postdoctoral Fellowship (No. SA046U16). The Japanese authors thank the financial support from MEXT (16H04106 for H.T. and 15H05754 for E.N.). The St Andrews team acknowledge support from the Engineering and Physical Sciences Research Council through grants EP/K503162/1 and EP/J009016/1. I.D.W.S. acknowledges a Royal Society Wolfson Research Merit Award.

Conflict of Interest

The authors declare no conflict of interest.

Keywords

conjugated polymers, distributed feedback lasers, oligomer, organic semiconductors

Received: January 19, 2018
Revised: March 1, 2018
Published online: April 10, 2018

[1] C. Grivas, *Prog. Quantum Electron.* **2016**, *3*, 45.
[2] A. J. C. Kuehne, M. C. Gather, *Chem. Rev.* **2016**, *116*, 12823.
[3] J. Clark, G. Lanzani, *Nat. Photonics* **2010**, *4*, 438.
[4] C. Vannahme, S. Klinkhammer, U. Lemmer, T. Mappes, *Opt. Express* **2011**, *19*, 8179.
[5] E. Heydari, J. Buller, E. Wischerchoff, A. Laschewsky, S. Döring, J. Stumpe, *Adv. Opt. Mater.* **2014**, *2*, 137.
[6] Y. Wang, P. O. Morawska, A. L. Kanibolotsky, P. J. Skabara, G. A. Turnbull, I. D. W. Samuel, *Laser Photonics Rev.* **2013**, *7*, L71.
[7] M. Morales-Vidal, P. G. Boj, J. A. Quintana, J. M. Villalvilla, A. Retolaza, S. Merino, M. A. Díaz-García, *Sens. Actuators B* **2015**, *220*, 1368.
[8] M. Morales-Vidal, P. G. Boj, J. M. Villavilla, J. A. Quintana, Q. Yan, N.-T. Lin, X. Zhu, N. Ruangsupapichat, J. Casado, H. Tsuji, E. Nakamura, M. A. Díaz-García, *Nat. Commun.* **2015**, *6*, 8458.
[9] J. A. Quintana, J. M. Villalvilla, M. Morales-Vidal, P. G. Boj, X. Zhu, N. Ruangsupapichat, H. Tsuji, E. Nakamura, M. A. Díaz-García, *Adv. Opt. Mater.* **2017**, 1700238.
[10] E. Nakamura, H. Tsuji, M. A. Díaz-García, M. Morales, P. G. Boj, J. M. Villalvilla J. A. Quintana, *Patent ES2547630*, **2016**.
[11] a) P. M. Burrezo, N.-T. Lin, K. Nakabayashi, S.-i. Ohkoshi, E. M. Calzado, P. G. Boj, M. A. Díaz García, C. Franco, C. Rovira, J. Veciana, M. Moos, C. Lambert, J. T. López Navarrete, H. Tsuji, E. Nakamura, J. Casado, *Angew. Chem., Int. Ed.* **2017**, *56*, 2898; b) P. M. Burrezo, X. Zhu, S.-F. Zhu, Q. Yan, J. T. López Navarrete, H. Tsuji, E. Nakamura, J. Casado, *J. Am. Chem. Soc.* **2015**, *137*, 3834; c) H. Nishioka, H. Tsuji, E. Nakamura, *Macromolecules*, in press, https://doi.org/10.1021/acs.macromol.8b00102.

[12] M. Gaal, C. Gadermaier, H. Plank, E. Moderegger, A. Pogantsch, G. Leising, E. J. W. List, *Adv. Mater.* **2003**, *15*, 1165.
[13] E. Mele, A. Camposeo, R. Stabile, P. Del Carro, F. Di Benedetto, L. Persano, R. Cingolani, D. Pisignano, *Appl. Phys. Lett.* **2006**, *89*, 131109.
[14] M. B. Christiansen, M. Schøler, A. Kristensen, *Opt. Express* **2007**, *15*, 3931.
[15] M. G. Ramírez, P. G. Boj, V. Navarro-Fuster, I. Vragovic, J. M. Villalvilla, I. Alonso, V. Trabadelo, S. Merino, M. A. Díaz-García, *Opt. Express* **2011**, *19*, 22443.
[16] G. Tsiminis, Y. Wang, A. L. Kanibolotsky, A. R. Inigo, P. J. Skabara, I. D. W. Samuel, G. A. Turnbull, *Adv. Mater.* **2013**, *25*, 2826.
[17] M. G. Ramírez, J. M. Villalvilla, J. A. Quintana, P. G. Boj, M. A. Díaz-García, *Opt. Mater. Express* **2014**, *4*, 733.
[18] J. R. C. Smirnov, Q. Zhang, R. Wannemacher, L. Wu, S. Casado, R. Xia, I. Rodríguez, J. Cabanillas-González, *Sci. Rep.* **2016**, *6*, 34565.
[19] N. Tsutsumi, S. Nagi, K. Kinashi, W. Sakai, *Sci. Rep.* **2016**, *6*, 34741.
[20] T. Zhai, X. Zhang, Z. Pang, *Opt. Express* **2011**, *19*, 6487.
[21] E. R. Martins, Y. Wang, A. L. Kanibolotsky, P. J. Skabara, G. A. Turnbull, I. D. W. Samuel, *Adv. Opt. Mater.* **2013**, *1*, 563.
[22] X. Zhu, H. Tsuji, J. T. López-Navarrete, J. Casado, E. Nakamura, *J. Am. Chem. Soc.* **2012**, *134*, 19254.
[23] M. D. McGehee, R. Gupta, S. Veenstra, E. K. Miller, M. A. Díaz-García, A. J. Heeger, *Phys. Rev. B* **1998**, *58*, 7035.
[24] R. Xia, G. Heliotis, Y. Hou, D. D. C. Bradley, *Org. Electron.* **2003**, *4*, 165.
[25] Y. Yang, G. A. Turnbull, I. D. W. Samuel, *Appl. Phys. Lett.* **2008**, *92*, 1.
[26] Y. Wang, G. Tsiminis, A. L. Kanibolotsky, P. J. Skabara, I. D. W. Samuel, G. A. Turnbull, *Opt. Express* **2013**, *21*, 14362.
[27] A. E. Vasdekis, M. J. Wilkins, J. W. Grate, R. T. Kelly, A. E. Konopka, S. S. Xantheas, T.-M. Chang, *Lab Chip* **2014**, *14*, 2072.
[28] G. L. Whitworth, S. Zhang, J. R. Y. Stevenson, B. Ebenhoch, I. D. W. Samuel, G. A. Turnbull, *Appl. Phys. Lett.* **2015**, *107*, 163301.